Charm meson and charm-meson molecule in an expanding hadron gas

Li-Ping He
Universität Bonn

Collaborators:
Eric Braaten, Roberto Bruschini, Kevin Ingles, Ohio State University
Jun Jiang, Shandong University

Based on arXiv:2209.04972, 2303.08072

Outline

Heavy-ion collisions: Overview

The standard model of heavy-ion collisions is a multi-stage model

S1 Initial Collision

- Impact parameter/centrality, energy deposition

S2 Thermalization

- Hydrodynamic/transport modeling

S3 Hadronization

- Hadron production at phase transition

S4 Kinetic freeze-out

- Hadrons stop interacting, momentum distributions frozen

State-of-the-art models consist of complex numerical simulations for each stage

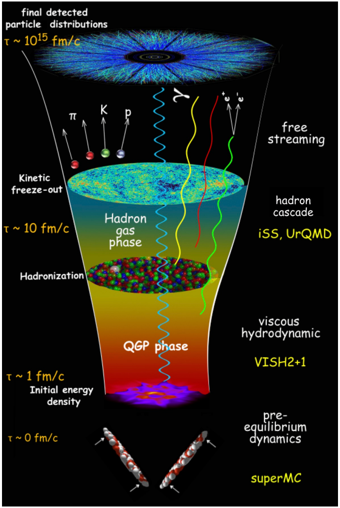

Credit: Chun Shen, Wayne State University

Heavy-ion collisions: Hadronization

At $T_H = 156$ MeV, quarks and gluons become confined to hadrons in process called "hadronization"

- A simple model for light hadron production: **Statistical Hadronization Model** (SHM)
  Abundance of light hadron is given by a Bose-Einstein distribution
- A simple model for charm hadron production: **SHMc**
  Abundance of charm hadron can be approximated by a relativistic Boltzmann distribution multiplied by charm-quark fugacity determined by the conservation of charm quark number

Andronic *et al.* NPA **772**, 167 (2006), JHEP **07**, 035 (2021), PLB **571**, 36 (2003)

Heavy-ion collisions: Kinetic freeze-out

At kinetic freeze-out, all interactions are assumed to stop.
A more appropriate assumption: the end of thermal equilibrium
(**hadron can continue to interact after kinetic freeze-out**)

The hadron gas can be approximated by a pion gas.

- temperature fixed at $T = T_F$
- volume continues to expand with proper time τ:

$$V(\tau) = \pi \left[R_F + v_F(\tau - \tau_F)\right]^2 c\tau$$

- pion number density decreases in inverse proportion to the volume:

$$\mathfrak{n}_\pi(\tau) = [V(\tau_F)/V(\tau)]\mathfrak{n}_\pi(\tau_F)$$

- pion momentum distributions are frozen and given by Bose-Einstein distributions with temperature T_F

Thermal mass shifts and widths: Charm mesons

In a pion gas, charm meson and pion properties are modified by the interactions with the pion gas.

D self-energy diagrams in HHχEFT at leading order

D^* self-energy diagrams in HHχEFT at leading order

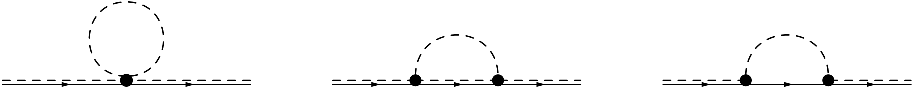

Thermal mass shifts and widths: Charm mesons

Thermal self-energies in a pion gas arise primarily from **coherent pion forward scattering**.

D self-energy diagrams from coherent pion forward scattering in HHχEFT at LO

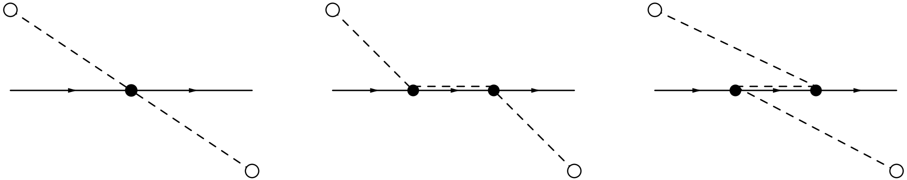

Thermal mass shifts and widths: Charm mesons

Thermal self-energies in a pion gas arise primarily from **coherent pion forward scattering**.

D^* self-energy diagrams from coherent pion forward scattering in HHχEFT at LO

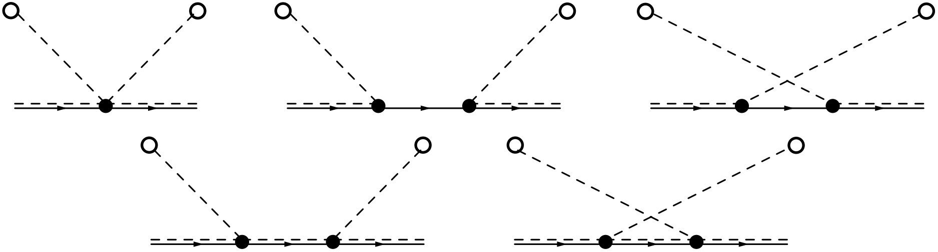

Thermal mass shifts and widths: Charm mesons

Real rest energies as functions of the temperature T

Real rest energy at T = real rest energy at $T = 0$ + thermal mass shift

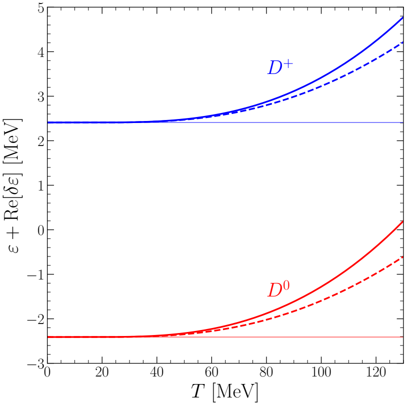

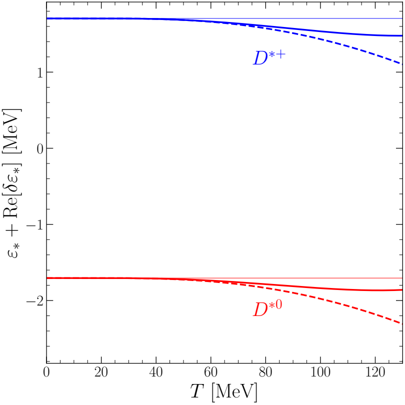

Dashed line: LO in heavy meson expansion ($m_\pi \ll M_D$)

Solid line: NLO in heavy meson expansion

Thermal mass shifts and widths: Charm mesons

Widths as functions of the temperature T

width at T = width at $T = 0$ + thermal width

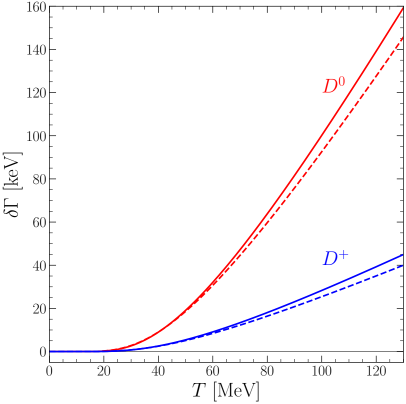

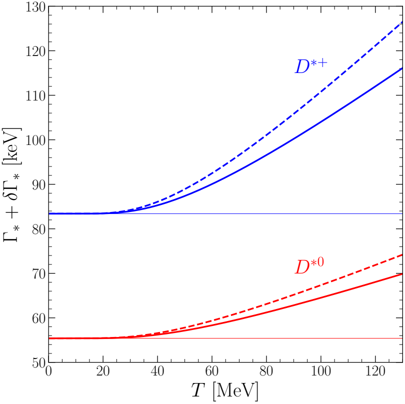

Dashed line: LO in heavy meson expansion

Solid line: NLO in heavy meson expansion

Thermal mass shifts and widths: Comparison with previous work

$\delta M - i\delta\Gamma$ for charm mesons in MeV.

T [MeV]	FMFK[1]		MRTT[2]	
	D	D^*	D	D^*
100	$-7-8i$	$-6-12i$	$-13-17i$	$-12-17i$
	CMR[3]		this work	
	D	D^*	D	D^*
100	$0-15i$	$0-10i$	$1.07-0.064i$	$-0.15-0.015i$

There are orders-of-magnitude discrepancies. Possible reasons:

- low-temperature constraints from chiral symmetry are violated in the previous work.

[1] Fuchs *et al.*, PRC **73**, 035204 (2006). [2] Montana *et al.*, PLB **806**, 135464 (2020), PRD **102**, 096020 (2020)
[3] Cleven *et al.*, PRC **96**, 045201 (2017)

Thermal mass shifts and widths: Comparison with previous work

Lattice QCD calculations of charm meson masses:
At $T = 47, 95, 109, 127$ MeV, the thermal mass shifts of D and D^* were consistent with 0.
At $T =$152 MeV, $\delta m_D = -20 \pm 7$ MeV, $\delta m_{D^*} = -43 \pm 10$ MeV.

Lattice QCD does not yet provide useful results for the thermal shifts in charm-meson masses at temperatures well below the hadronization temperature.

Aarts *et al.*, arXiv:2209.14681

Thermal mass shifts and widths: Charm mesons

Thermal widths VS pion number density

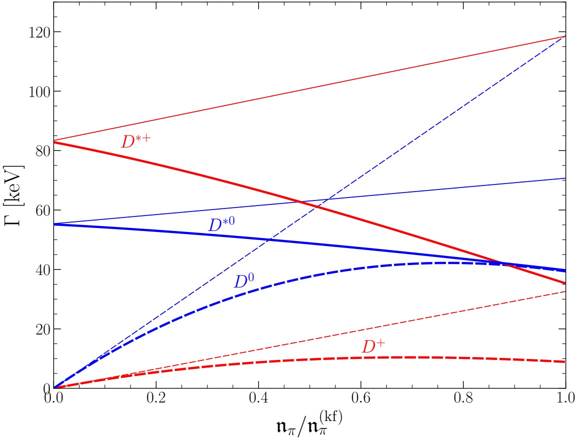

thicker (thinner) lines: widths with mass shift (not) taken into account

Evolution of charm-meson abundances: Overview

All previous studies have assumed that D^* just decays after kinetic freeze-out but has no other interactions

D^{*0} decays into D^0 at 100%
D^{*+} decays into D^0 at B_{+0} and D^+ at $1 - B_{+0}$ ($B_{+0} = 0.677 \pm 0.005$)

Naïve equations for final charm-meson abundances are

$$N_0 = (N_0)_0 + (N_{*0})_0 + B_{+0}\,(N_{*+})_0$$
$$N_+ = (N_+)_0 + 0\,(N_{*0})_0 + (1 - B_{+0})\,(N_{*+})_0$$

SHMc predictions gives $(N_0/N_+)_{\text{naïve}} = 2.256 + 0.014$, the error-bar is only from B_{+0}

Andronic *et al.* JHEP **07**, 035 (2021)

Evolution of charm-meson abundances: t-channel singularities

We exploit the fact that charm mesons still interact after kinetic freeze-out

(a) $D^{*a} \longleftrightarrow \pi D^b$

(b) $\pi D^a \longleftrightarrow \pi D^b$

(c) $\pi D^{*a} \longleftrightarrow \pi D^b$

(d) $\pi D^{*a} \longleftrightarrow \pi D^{*b}$, $\cdots$

There are t-channel singularities in the reaction $\pi D^* \to \pi D^*$

Definition

A t-channel singularity is a divergence in the rate of a reaction in which an unstable particle decays and one of its decay products scatters. The divergence arises if the exchanged particle can be on-shell.

Evolution of charm-meson abundances: t-channel singularities

t-channel singularities were first discussed by Peierls in 1961 for πN^* scattering

In the diagram, the exchanged nucleon N can be on shell because the N^* can decay into $N\pi$. This leads to a divergence in the cross section

Peierls suggested that the N^* width be inserted into N propagator
However, this still leads to unphysically large cross sections

Peierls, PRL **6**, 641-643 (1961)

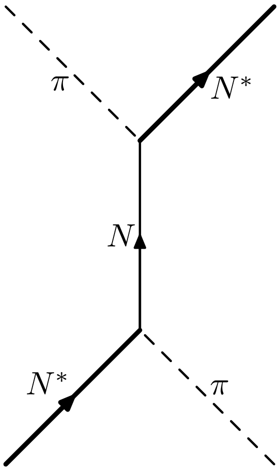

t-channel singularities

Charm-meson reaction $\pi D^* \to \pi D^*$ can have t-channel singularity because the exchanged D can be on-shell

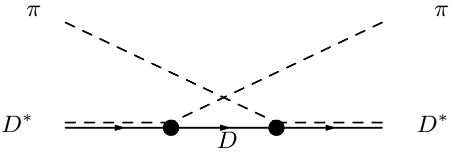

In the case of elastic scattering, the t-channel singularity region is

$$2M_*^2 - M^2 + 2m^2 < s < \left(M_*^2 - m^2\right)^2 / M^2$$

Interval in $\sqrt{s}$ for $\pi^0 D^{*0} \to \pi^0 D^{*0}$ is 2 MeV .

For production in heavy-ion collisions, t-channel singularities can be regularized by thermal width of D

$$\text{cross section} \propto \frac{1}{\text{thermal width}} : \langle v\sigma[\pi D^{*+}, \pi D^{*0}]\rangle = \frac{1}{3\mathfrak{n}_\pi} \frac{\Gamma_{*0,0}\Gamma_{*+,0}}{\Gamma_{*0,0} + \Gamma_{*+,0}}$$

Evolution of charm-meson abundances

Full evolution equations

$$\mathfrak{n}_\pi \frac{d}{d\tau}\left(\frac{\mathfrak{n}_a}{\mathfrak{n}_\pi}\right) = [1 + f_\pi(\Delta)] \sum_b \Gamma_{*b,a}\mathfrak{n}_{*b} + \Gamma_{*a,\gamma}\mathfrak{n}_{*a} - 3\sum_b \langle v\sigma_{\pi a,*b}\rangle \mathfrak{n}_a \mathfrak{n}_\pi$$
$$+ 3\sum_{a\neq b}\langle v\sigma_{\pi a,\pi b}\rangle(\mathfrak{n}_b - \mathfrak{n}_a)\mathfrak{n}_\pi$$
$$+ 3\sum_b \left(\langle v\sigma_{\pi * b,\pi a}\rangle \mathfrak{n}_{*a} - \langle v\sigma_{\pi a,\pi * b}\rangle \mathfrak{n}_a\right)\mathfrak{n}_\pi + \cdots$$

$$\mathfrak{n}_\pi \frac{d}{d\tau}\left(\frac{\mathfrak{n}_{*a}}{\mathfrak{n}_\pi}\right) = 3\sum_b \langle v\sigma_{\pi b,*a}\rangle \mathfrak{n}_b \mathfrak{n}_\pi - \left([1 + \mathfrak{f}_\pi(\Delta)] \sum_b \Gamma_{*b,a} + \Gamma * a, \gamma\right)\mathfrak{n}_{*a}$$
$$+ 3\sum_b \left(\langle v\sigma_{\pi b,\pi * a}\rangle \mathfrak{n}_b - \langle v\sigma_{\pi * a,\pi b}\rangle \mathfrak{n}_{*a}\right)\mathfrak{n}_\pi$$
$$+3\sum_{b\neq a}\langle v\sigma_{\pi * b,\pi * a}\rangle(\mathfrak{n}_{*b} - \mathfrak{n}_{*a})\mathfrak{n}_\pi + \cdots$$

where, for example $\langle v\sigma_{\pi a,*b}\rangle \longleftrightarrow \langle v\sigma[\pi D^a \to D^{*b}]\rangle$

Evolution of charm-meson abundances

Using initial conditions provided by the predictions from SHMc

$$(N_0/N_\pi, N_+/N_\pi, N_{*0}/N_\pi, N_{*+}/N_\pi)_0 = 10^{-3}(2.76,\, 2.64,\, 3.37,\, 3.28)$$

Fractions: f_{D^0} (blue), f_{D^+} (red), $f_{D^{*0}}$ (cyan), and $f_{D^{*+}}$ (magenta)

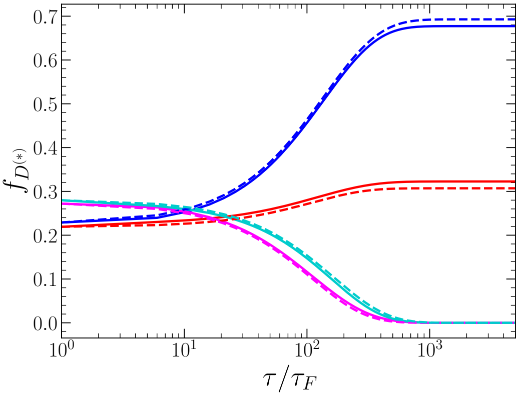

$N_0/N_+ = 2.100$ **at the detector, differs from** $(N_0/N_+)_{\text{naïve}} = 2.256 + 0.014$ **by** 11σ**.**

Evolution of charm-meson abundances

At late times, $\mathfrak{n}_\pi \ll 10^{-3}\mathfrak{n}_\pi^{(\mathrm{eq})}$, the only terms that remain in the evolution equations are 1-body terms:

- decay terms
- t-channel singularities: e.g. reaction rate $\langle v\sigma_{\pi*+,\pi*0}\rangle$ for $\mathfrak{n}_\pi \to 0$ has form
$$\langle v\sigma[\pi D^{*+}, \pi D^{*0}]\rangle = \frac{1}{3\mathfrak{n}_\pi}\frac{\Gamma_{*0,0}\Gamma_{*+,0}}{\Gamma_{*0,0}+\Gamma_{*+,0}}$$
factor $1/\mathfrak{n}_\pi$ cancels with $\mathfrak{n}_\pi$ in evolution equations

Resulting system of differential equations can be solved exactly.
Difference between naïve prediction and analytic prediction with the t-channel singularity is significantly different from 0 at 13σ:

$$\left(\frac{N_0}{N_+}\right)_{\text{naïve}} - \left(\frac{N_0}{N_+}\right)_{\text{analytic}} = 0.079 \pm 0.006$$

errors come from $B_{+0}, B_{00}, \Gamma_{*+}$ and Γ_{*0}

Loosely bound charm-meson molecule: Overview

amplitude for the propagation of D and D^* between contact interactions

in vacuum:

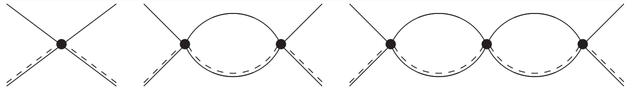

$$= \frac{i(2\pi/\mu)}{\frac{2\pi/\mu}{C_0} - \Lambda + S_0(E_{\rm cm})} = \frac{i\,(2\pi/\mu)}{-\gamma_X + S_0(E_{\rm cm})}$$

If the binding momentum $\gamma_X > 0$, it has a pole at $E_{\rm cm} = E_X = -\gamma_X^2/(2\mu)$

in a hadron gas:

$$\frac{i\,(2\pi/\mu)}{\frac{2\pi/\mu}{C_1} - \Lambda + S_0(E_{\rm cm}) + \Sigma(E_{\rm cm}, P)} \to \frac{i\,(2\pi/\mu)\,Z_X}{-(\gamma_X + \delta\gamma_X) + S_1(E_{\rm cm}, P) + \dots}$$

$$S_0(E_{\rm cm}) = \sqrt{-2\mu\Big[E_{\rm cm} - (\varepsilon_* + \varepsilon) + i\epsilon\Big]}, \quad S_1(E_{\rm cm}) = \sqrt{-2\mu\Big[E_{\rm cm} + i\epsilon + \dots\Big]}$$

Loosely bound charm-meson molecule: Self-energy

One-loop diagrams for $\Sigma(E_{\rm cm}, P)$ from coherent pion forward scattering

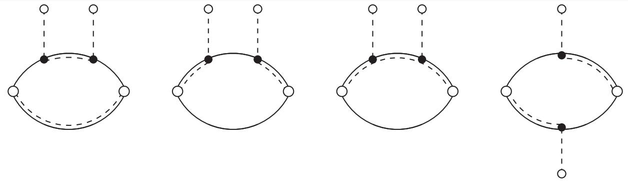

Two-loop diagram for $\Sigma(E_{\rm cm}, P)$ from coherent pion forward scattering

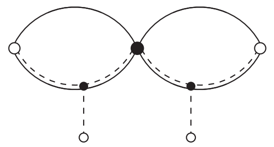

Loosely bound charm-meson molecule: Self energy

Contact vertex corrections: δC

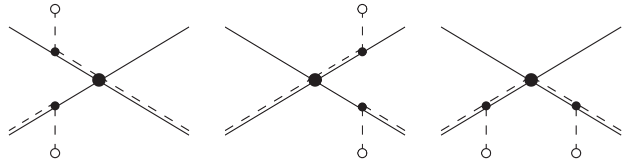

complete amplitude in a pion gas:

$$\frac{i\,(2\pi/\mu)}{\frac{2\pi/\mu}{C_1} - \Lambda + S_0(E_{\rm cm}) + \Sigma(E_{\rm cm}, P)} = \frac{i\,(2\pi/\mu)\,Z_X}{-(\gamma_X + \delta\gamma_X) + S_1(E_{\rm cm}, P) + \ldots}$$

$$S_1(E_{\rm cm}, P) = \sqrt{-2\mu\left[E_{\rm cm} - (\varepsilon_* + \varepsilon) - (\delta\varepsilon_* + \delta\varepsilon) - \zeta_X P^2/(2M_X) + i\epsilon\right]}$$

Loosely bound charm-meson molecule: Thermal mass shifts and widths

Pole energy of molecule with zero 3-momentum at NLO:

$$E_X = (\varepsilon_{*a} - i\,\Gamma_{*a}/2) + \varepsilon_b + (\delta\varepsilon_{*a} + \delta\varepsilon_b) - (\gamma_X + \delta\gamma_X)^2/(2\mu).$$

$\delta\varepsilon_{*a}, \delta\varepsilon_b$: thermal energy shift for charm mesons
$\delta\gamma_X$: correction to the binding momentum

$X(3872)$ pole energy from LHCb: $(0.025 - 0.140i)$ MeV
$X(3872)$ pole energy in a pion gas at $T = 115$ MeV: $(1.64 - 0.21i)$ MeV

$T_{cc}^{+}(3875)$ pole energy from LHCb: $(-0.36 - 0.024i)$ MeV
$T_{cc}^{+}(3875)$ pole energy in a pion gas at $T = 115$ MeV: (1.20 - 0.10 i) MeV

Thermal contribution from correction to the binding momentum is negligible compared to those from charm meson constituents

LHCb, JHEP **08**, 123 (2020)
LHCb, Nature Commun. **13**, 3351(2022)

Loosely bound charm-meson molecule: Thermal mass shifts and widths

Pole energy of molecule with zero 3-momentum at NLO:

$$E_X = (\varepsilon_{*a} - i\,\Gamma_{*a}/2) + \varepsilon_b + (\delta\varepsilon_{*a} + \delta\varepsilon_b) - (\gamma_X + \delta\gamma_X)^2/(2\mu).$$

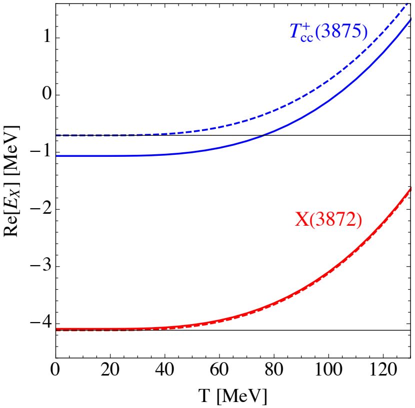

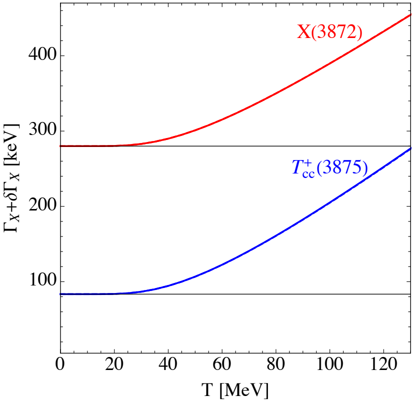

Dashed lines: charm-meson thresholds

Loosely bound charm-meson molecule: Comparison with previous work

Thermal mass shifts and widths for $X(3872)$ at $T = 100$ MeV

	$M_X - M_{DD^*}^{T=0}$	δM_{DD^*}	$\delta\Gamma_X$	$M_X - M_{DD^*}$ at $T = 0$
CMR[1] [MeV]	$+3$	0	30	-2.5
MRTT[2] [MeV]	-30	-27	30	-4
This work	0.97	1.00	0.11	0.025

There are orders-of-magnitude discrepancies. Possible reasons:

- low-temperature constraints from chiral symmetry are violated in the previous work.

[1] Cleven *et al.*, PLB **799**, 135050 (2019): the $D^* D$ threshold was somehow held constant at its $T = 0$ value
[2] Montana *et al.*, arXiv:2211.01896

Prompt production of X(3872) in PbPb collisions

CMS, Phys. Rev. Lett. **128**, 032001 (2022)

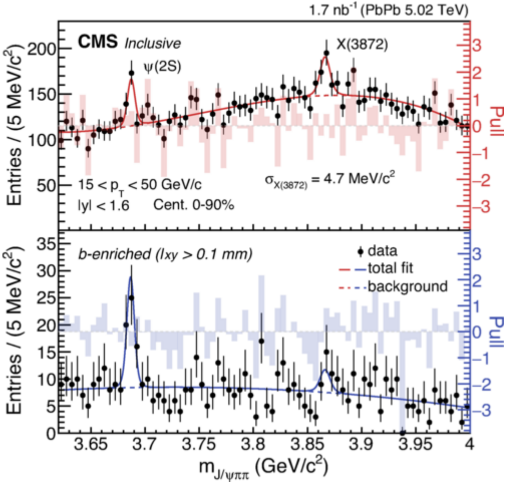

prompt X-to-ψ' ratio ~ 1, order of magnitude larger than in pp collisions

Summary

(a) We calculated the thermal mass shifts and widths of $D^{(*)}$ mesons to NLO in the heavy-meson expansion

(b) We have identified an aspect of charm-meson physics in which the effects of the t-channel singularity is observable

(c) Our findings provide encouragement to study other effects of t-channel singularities, such as in the production of loosely bound charm-meson molecules in heavy-ion collisions

(d) Thermal corrections to a loosely bound charm-meson molecule in a pion gas come primarily from the complex thermal energy shift of the charm-meson constituents.

(e) It is encouraging to observe loosely bound charm-meson molecules in the hadron gas from the heavy-ion collisions.

Thank you for your attention.